

Perfluorinated Alkoxyaluminate Salts of Cationic Brønsted Acids: Synthesis, Structure, and Characterization of $[\text{H}(\text{OEt}_2)_2][\text{Al}\{\text{OC}(\text{CF}_3)_3\}_4]$ and $[\text{H}(\text{THF})_2][\text{Al}\{\text{OC}(\text{CF}_3)_3\}_4]$

Ingo Krossing^{*[a,b]} and Andreas Reisinger^[a,b]

Keywords: Acidity / Aluminum / Brønsted acids / IR spectroscopy / Hydrogen bonds

The strong cationic Brønsted acids $[\text{H}(\text{OEt}_2)_2][\text{Al}\{\text{OC}(\text{CF}_3)_3\}_4]$ (**1**) and $[\text{H}(\text{THF})_2][\text{Al}\{\text{OC}(\text{CF}_3)_3\}_4]$ (**2**) were prepared in up to 95 % yield by reacting stoichiometric amounts of diethyl ether/THF solutions of $\text{Li}[\text{Al}\{\text{OC}(\text{CF}_3)_3\}_4]$ and HX ($\text{X} = \text{Cl}, \text{Br}$), removing the solvent, and extracting the residue with CH_2Cl_2 . Compounds **1** and **2** were characterized by multinuclear NMR and IR spectroscopy as well as by their single crystal X-ray structures and additional quantum chemical calculations. The cation in **1** probably contains an unsymmetrical $\text{O}\cdots\text{H}\cdots\text{O}$ hydrogen bond, while in **2** the protic hydrogen atom was not found in the difference Fourier map. From an analysis of all published $[\text{H}(\text{OEt}_2)_2]^+$ structures, we show that

for an unsymmetrical H-bridge further rearrangement of the structure occurs leading to the structural type **III** that may formally be viewed as ethanol coordinating to an ethyl cation. This point of view has hitherto been neglected in the discussion of the nature of short, strong, low-barrier H-bonds, although it needs to be accounted for. Both **1** and **2** are suitable starting materials to introduce the weakly coordinating and chemically very robust $[\text{Al}\{\text{OC}(\text{CF}_3)_3\}_4]^-$ anion by protonolysis.

(© Wiley-VCH Verlag GmbH & Co. KGaA, 69451 Weinheim, Germany, 2005)

Introduction

Salts of protonated ether solvents in superacidic solutions have been known for about 40 years.^[1] In 1985 an isolated report of the structure of $[\text{H}(\text{OEt}_2)_2][\text{Zn}_2\text{Cl}_6]$ appeared,^[2] but in recent years salts of the oxonium acids $[\text{H}(\text{OEt}_2)_2]^+$ and $[\text{H}(\text{THF})_2]^+$ with several weakly coordinating anions (WCAs),^[3] such as $[\text{BAr}^{\text{F}}_4]^-$ [$\text{Ar}^{\text{F}} = \text{C}_6\text{F}_5$,^[4] $\text{C}_6\text{H}_3(\text{CF}_3)_2$,^[5,6] $[\text{CHB}_{11}\text{R}_5\text{X}_6]^-$ ($\text{R} = \text{H}, \text{CH}_3$; $\text{X} = \text{Cl}, \text{Br}$),^[7] $[(\text{F}_5\text{C}_6)_3\text{B}(\mu\text{-X})\text{B}(\text{C}_6\text{F}_5)_3]^-$ ($\text{X} = \text{C}_3\text{N}_2\text{H}_3^-$,^[8] NH_2^- ,^[9]) or $[\text{C}_6\text{F}_4\text{-1,2-}\{\text{B}(\text{C}_6\text{F}_5)_2\}_2(\mu\text{-OCH}_3)]^-$ ^[10] have been prepared and characterized by different spectroscopic methods as well as X-ray crystallography. $[\text{H}(\text{OEt}_2)_2]^+$ salts in particular have emerged as very versatile reagents in organometallic synthesis and catalysis.^[4–10,11] However, all the currently known $[\text{H}(\text{OEt}_2)_2]^+$ salts are hampered by either their low thermal solution stability [i.e. $[\text{H}(\text{OEt}_2)_2][\text{BAr}^{\text{F}}_4]$ [$\text{Ar}^{\text{F}} = \text{C}_6\text{H}_3(\text{CF}_3)_2$]] or difficulties in obtaining the starting materials due to the need to intermediately prepare explosive

$\text{C}_6\text{F}_5\text{Li}$ or the carborane anions. Thus, there is demand for further, easily accessible and in solution thermally stable $[\text{H}(\text{OEt}_2)_2]^+$ salts.

Recently, we reported the facile preparation of nonoxidizing weakly coordinating anions of type $[\text{Al}(\text{OR}^{\text{F}})_4]^-$ [$\text{R}^{\text{F}} = \text{CH}(\text{CF}_3)_2$, $\text{C}(\text{CH}_3)(\text{CF}_3)_2$, $\text{C}(\text{CF}_3)_3$]^[12,13] and their use to stabilize weakly bound silver complexes such as $\text{Ag}(\eta^2\text{-P}_4)_2^+$ ^[14] and $\text{Ag}(\eta^4\text{-S}_8)_2^+$ ^[15] as well as highly electrophilic cations like PX_4^+ , P_2X_5^+ , P_3I_6^+ , and P_5X_2^+ ($\text{X} = \text{Br}, \text{I}$),^[16,17] CS_2Br_3^+ ,^[18] and Cl_3^+ ,^[19] Li^+ ,^[12,13] Ag^+ ,^[12] Tl^+ ,^[20] Cs^+ , Ph_3C^+ ,^[21] and NR_4^+ ^[13,22] salts of these anions are available as starting materials; however, cationic Brønsted acids with the $[\text{Al}(\text{OR}^{\text{F}})_4]^-$ anions are still unknown.

Herein we report the synthesis and characterization of $[\text{Al}(\text{OR}^{\text{F}})_4]^-$ salts [$\text{R}^{\text{F}} = \text{C}(\text{CF}_3)_3$] of the oxonium acids $[\text{H}(\text{OEt}_2)_2]^+$ and $[\text{H}(\text{THF})_2]^+$. Due to their facile access, the commercial availability of $\text{Li}[\text{Al}(\text{OR}^{\text{F}})_4]$ (Strem) as well as the weakly coordinating and stable counterion, these compounds are a good alternative to the widely used $[\text{H}(\text{OEt}_2)_2][\text{BAr}^{\text{F}}_4]$ salts. Moreover, during the last ten years a considerable experimental and theoretical debate has been going on as to whether a truly symmetrical hydrogen bond exists or not.^[7,23] A complete understanding and proof of one of the models has still not been achieved and the nature of these short, strong, low-barrier H-bonds remains somewhat unclear.

[a] Universität Karlsruhe, Institut für Anorganische Chemie, Engesserstr. Geb. 30.45, 76128 Karlsruhe, Germany

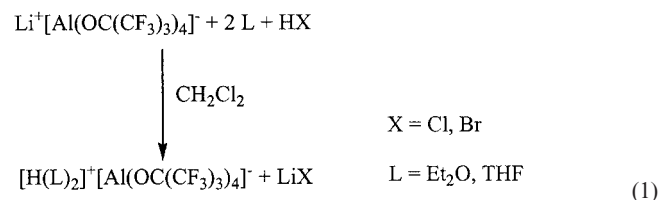
[b] Present address: Ecole Polytechnique Fédérale de Lausanne (EPFL), Laboratory of Inorganic and Coordination Chemistry (LCIC), ISIC-BCH, 1015 Lausanne, Switzerland
E-mail: ingo.krossing@epfl.ch

Supporting information for this article is available on the WWW under <http://www.eurjic.org> or from the author.

Results and Discussion

Synthesis

$\text{LiAl}[\text{OC}(\text{CF}_3)_3]_4$ was prepared by reaction of LiAlH_4 with $\text{HOC}(\text{CF}_3)_3$ in toluene.^[12,13] The Li salt was suspended in CH_2Cl_2 and treated with diethyl ether/THF solutions of HX ($\text{X} = \text{Cl}, \text{Br}$) to produce precipitation of LiX . The products $[\text{H}(\text{OEt}_2)_2][\text{Al}\{\text{OC}(\text{CF}_3)_3\}_4]$ (**1**) and $[\text{H}(\text{THF})_2][\text{Al}\{\text{OC}(\text{CF}_3)_3\}_4]$ (**2**) were isolated after work-up in up to 95% yield [Equation (1)].



Compound **1** was obtained as a white powder by redissolving the residue from the reaction in CH_2Cl_2 . This air- and moisture-sensitive powder is stable at room temperature and soluble in several moderately polar organic solvents, such as diethyl ether, diethyl ether/toluene mixtures, chloroform, dichloromethane, and 1,2-dichloroethane. Solutions of **1** in CD_2Cl_2 are stable for at least a week at ambient temperature. Solid **1** is stable for several months at room temperature and may be heated up to 75 °C without alteration (DTA analysis); further heating causes decomposition. In the DTA trace only variations of the gradient at 103 °C (18% weight loss) and 148 °C (further 60% weight

loss) can be observed, with no distinct steps. From other DTA traces, and the fact that $\text{LiAl}[\text{OC}(\text{CF}_3)_3]_4$ can be sublimed at about 130–140 °C without decomposition,^[12] it seems likely that the decomposition starts with the loss of two diethyl ether molecules (18% obsvd. weight loss vs. theoretical value of 13%). However, it cannot be excluded that $\text{HOC}(\text{CF}_3)_3$ and one molecule of OEt_2 are ejected first to leave $\text{Et}_2\text{O} \cdot \text{Al}[\text{OC}(\text{CF}_3)_3]_3$ as a nonvolatile residue. The second step between 100 °C and 150 °C results from decomposition of the anion. During that decomposition one equivalent of $\text{HOC}(\text{CF}_3)_3$ and two equivalents of $\text{F}_2\text{COC}(\text{CF}_3)_2$ are presumably formed, in agreement with a total weight loss of 60% (theory: 60%), to leave the relatively stable $\text{AlF}_2(\text{OR})$. Further decomposition and weight loss is slow and spread over 200 °C. The observed weight loss is in agreement with the formation of another equivalent of the epoxide $\text{F}_2\text{COC}(\text{CF}_3)_2$ (exp. 13%; theory 19%). This results in a total weight loss of 91% (theoretical value: 92%) and the formation of nonvolatile AlF_3 at approximately 350 °C. Figure 1 shows a likely route for the thermal decomposition and the differential temperature analysis of **1** between 30 and 350 °C.

The preparation of **2** is less straightforward. After filtration and removal of all volatiles an oily brown residue remained that probably contains THF polymerization products^[7] in addition to the product **2**, which is the major component (approx. 80% of the oil, by NMR spectroscopy). Compound **2** crystallized as less-rhombus-shaped crystals in good yield (65%) within two days directly from this oily residue. The crystals were isolated from the oil by decantation followed by several washings with pentane. Crystalline air- and moisture-sensitive **2** is stable at room temperature and soluble in the same solvents as **1** (see above).

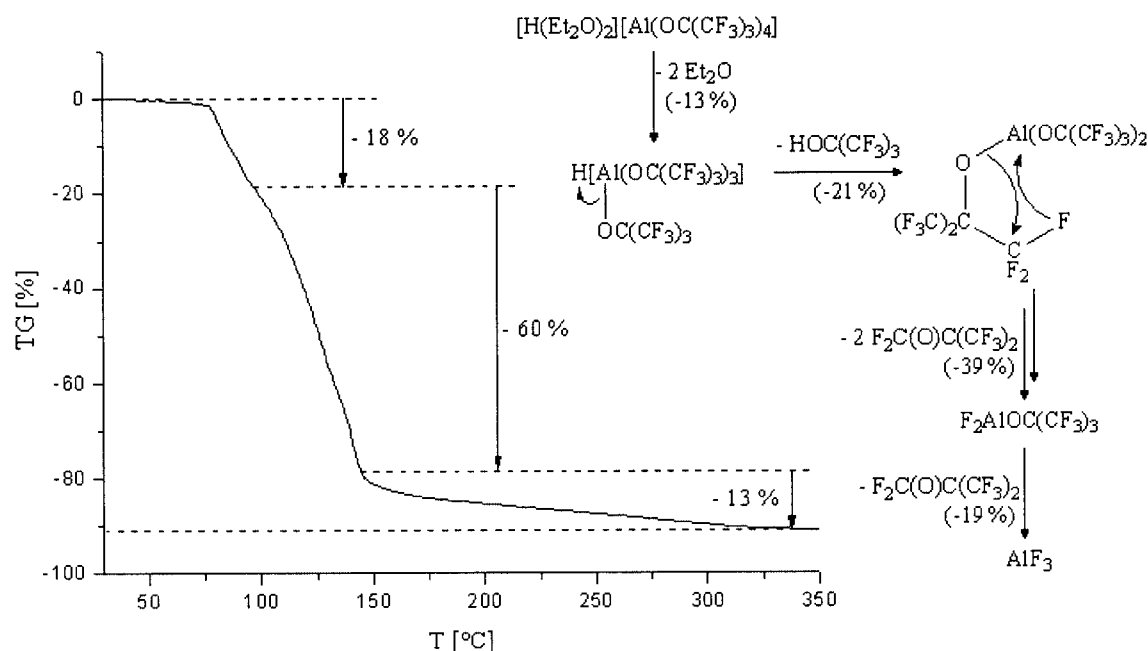
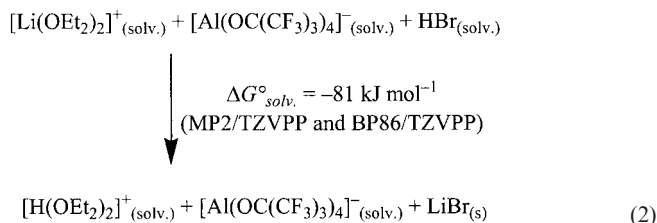


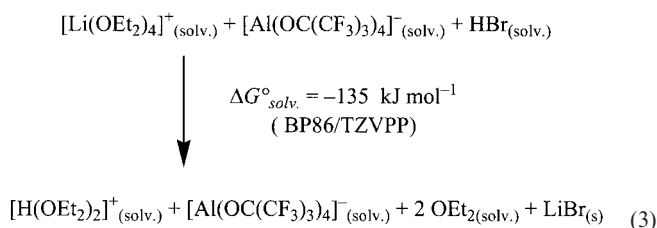
Figure 1. DTA analysis of **1** between 30 and 350 °C (left) and hypothetical route for the decomposition (right).

Thermodynamics of the Formation of 1

We assessed the driving force for the formation of **1** in more detail. Assuming that the isodesmic reaction (2) takes place in CH₂Cl₂, it is possible to reliably obtain its reaction enthalpy by quantum chemical calculations (see computational details). The part of the anion cancels.



As expected for an isodesmic reaction, BP86/TZVPP (DFT) and MP2/TZVPP (ab initio) calculations agree on the same value for $\Delta G^\circ_{\text{solv.}}$ of -81 kJ mol^{-1} . However, for the calculations to form an isodesmic reaction, Equation (2) assumes that the rather odd $\text{Li}(\text{OEt}_2)_2^+$ cation is present in solution. However, the cation $\text{Li}(\text{OEt}_2)_4^+$ is more likely, as shown by various crystal structures of $\text{Li}(\text{L})_4^+$ salts (L = ethereal solvent).^[8] Therefore, we assessed reaction (3), which is no longer isodesmic and thus $\Delta G^\circ_{\text{solv.}}$ may be less accurate; however, the species presented in (3) are very close to the situation actually taking place in solution.



Again, the part of the anion cancels. Equation (3) is additionally favored by entropy due to the release of two ether molecules. $\Delta G^\circ_{\text{solv.}}$ of this reaction is exergonic by

-135 kJ mol^{-1} and is thus very favorable, in agreement with the facile preparation of **1**. We assume a similar situation for **2**, although this is not explicitly discussed.

NMR Spectroscopy

Protonated Diethyl Ether Moiety

The ¹⁹F and ²⁷Al NMR spectroscopy show one characteristic sharp signal for the intact counterion. In the ¹H NMR spectrum a broad downfield-shifted signal at $\delta = 18.2 \text{ ppm}$ (OH) and signals for the CH₃ and CH₂ protons of the coordinating diethyl ether molecules are observed. The OH signal varies greatly from sample to sample, with values between $\delta = 14.5$ and 18.2 ppm . The integration of the signals shows the constitution as two coordinated diethyl ether molecules per proton, similar to all the earlier synthesized etherates.^[4–10] Compared to free diethyl ether,^[24] these two signals are slightly shifted downfield (Table 1). The ¹³C NMR spectrum shows the signals of the anion and two signals which were assigned to the methyl and methylene groups of the cation. In Table 1, the observed ¹H and ¹³C signals of the cation are collected and compared to different salts of $[\text{H}(\text{OEt}_2)_2]^+$ as well as the shifts calculated by DFT.

In the article^[10] on $[\text{H}(\text{OEt}_2)_2][\text{C}_6\text{F}_4\text{-1,2-}\{\text{B}(\text{C}_6\text{F}_5)_2\}_2(\mu\text{-OCH}_3)]$, the ¹³C signal at $\delta = 57.9 \text{ ppm}$ was assigned to the methylene group of the cation. Since all the other data of this signal, including the DFT calculations, range from $\delta = 67.8$ to 70.4 ppm it was probably incorrectly assigned. The authors also observed one signal at $\delta = 69.0 \text{ ppm}$ which was assigned to the methoxy group of the anion;^[10] however, the collection of chemical shifts in Table 1 clearly indicates that this assignment is erroneous and the shifts must be reversed, i.e. the signal at $\delta = 69.0 \text{ ppm}$ belongs to the CH₂ group of protonated diethyl ether and the signal at $\delta = 57.9 \text{ ppm}$ to the methoxy group of the anion.

¹H and ¹³C solid-state MAS NMR measurements matched with the solution spectra: in the ¹H NMR spectrum signals are observed at $\delta = 1.32, 3.90$ and 16.6 ppm . Apart from the typical anion signals,^[12] the ¹³C NMR spectrum shows one signal at $\delta = 12.7 \text{ ppm}$ and two signals at $\delta = 71.1$ and 71.6 ppm . None of these signals can be assigned to free diethyl ether since that signal has a chemical shift of $\delta = 65.2 \text{ ppm}$.^[24] This suggests an asymmetric envi-

Table 1. Comparison of the ¹H and ¹³C chemical shifts of $[\text{H}(\text{OEt}_2)_2]^+$ salts with different anions and shifts calculated by DFT [BP86/SV(P)].

| | $[\text{Al}\{\text{OC}(\text{CF}_3)_3\}_4]$ | $[\text{B}(\text{C}_6\text{F}_5)_4]^{[4]}$ | $[\text{C}_6\text{F}_4\text{-1,2-}\{\text{B}(\text{C}_6\text{F}_5)_2\}_2(\mu\text{-OCH}_3)]^{[10]}$ | $[\text{CHB}_{11}\text{R}_5\text{X}_6]^{[7]}$ | (BP86/SV(P)) |
|---------------------------------------|---|--|---|---|--------------|
| $\delta_{\text{H}}(\text{CH}_3)$ | 1.34/1.32 ^[a] | 1.42 | 1.43 | 0.78 | 1.2 |
| $\delta_{\text{H}}(\text{CH}_2)$ | 3.90/3.90 ^[a] | 7.55 ^[b] | 4.08 | 3.32 | 3.5 |
| $\delta_{\text{H}}(\text{OH})$ | 18.2/16.6 ^[a] | 15.5 | 16.4 | 13.8 | 12.8 |
| $\delta_{^{13}\text{C}}(\text{CH}_3)$ | 13.8/12.7 ^[a] | 13.9 | 14.5 | – | 16.8 |
| $\delta_{^{13}\text{C}}(\text{CH}_2)$ | 69.9/71.1–71.7 ^[a] | 70.4 | 69.0 | – | 75.1 |

^[a] Solution/MAS NMR spectroscopy. ^[b] Since this value differs from all other experimental and calculated shifts, it is erroneous.

ronment of the two coordinated ether molecules in the solid state.

Protonated THF

NMR spectroscopy gave the expected sets of signals that match with the DFT calculations and that of the only other reported compound ($[\text{H}(\text{THF})_2][\text{CHB}_{11}\text{R}_5\text{X}_6]$, Table 2).^[7]

Table 2. Comparison of NMR shifts of $[\text{H}(\text{THF})_2]^+$ with two anions and shifts calculated by DFT.

| | $[\text{H}(\text{THF})_2]\text{-}[\text{Al}\{\text{OC}(\text{CF}_3)_3\}_4]$ | $[\text{H}(\text{THF})_2]\text{-}[\text{CHB}_{11}\text{R}_5\text{X}_6]$ ^[7] | BP86/SV(P) |
|-------------------------------------|---|--|------------|
| $\delta_{\text{H}}(\text{CH}_2)$ | 2.05 | 1.30 | 1.9 |
| $\delta_{\text{H}}(\text{OCH}_2)$ | 3.95 | 3.60 | 3.6 |
| $\delta_{\text{H}}(\text{OH})$ | ≈ 8, broad (exchange?) | 14.80 | 13.1 |
| $\delta_{13\text{C}}(\text{CH}_2)$ | 25.5 | – | 29.1 |
| $\delta_{13\text{C}}(\text{OCH}_2)$ | 70.6 | – | 73.8 |

Vibrational Spectroscopy

The IR spectrum of **1**, especially the portion shown in Figure 2, exhibits the typical bands of the perfluorinated aluminate anion in the range between 286 and 1353 cm^{-1} . They can easily be assigned by comparison with other salts of this anion as well as with the calculated vibrational frequencies, as demonstrated in Table 3. The most characteristic anion vibrations are the very strong bands at 727 and 973 cm^{-1} as well as those between 1219 and 1353 cm^{-1} . The fact that the positions of the anion bands remain unchanged relative to the calculated frequencies and the NEt_4^+ salt indicates that there is no coordination of the

anion as, for example, occurs with the naked Li^+ or Ag^+ cation. The anion bands of the Raman spectrum of **1** match well with the IR spectrum. The most important differences between the spectra arise from the two strong bands at 744 and 798 cm^{-1} and the absence of the very strong IR bands in the range between 1200 and 1320 cm^{-1} , as can be seen in Table 3.

The remaining bands of the IR spectrum at $\tilde{\nu} = 769, 907, 1013, 1063, 1092, 1166, 1366$, and 1536 cm^{-1} can now be assigned to vibrations of the cation. Table 4 shows the experimental bands compared to the carboranate anion of Reed,^[7] the maxima of the simulated calculated cation spectrum, as well as the experimental^[25] and calculated bands of free diethyl ether in the range between 700 and 3000 cm^{-1} . This table also contains an assignment of the calculated bands and the related experimental modes. Compared to the calculated frequencies, the experimental bands match well. The expected bands at 726, 1212, 1312, and around 3000 cm^{-1} are likely overlapped by strong anion or Nujol bands. As already noted earlier, the cation bands are rather broad.^[7,23] Similarly to Reed's $[\text{H}(\text{OEt}_2)_2]\text{-}[\text{CHB}_{11}\text{H}_5\text{Cl}_6]$ salt, the very strong sharp $\nu_{\text{as}}(\text{C-O-C})$ band of free Et_2O (1120 cm^{-1}) disappears.^[7]

The Raman spectrum of **1** obtained at low temperature shows several bands in the range between 2850 and 3010 cm^{-1} which can be assigned with no doubt to C–H vibrations of the cation. At lower energy two bands at 1467 and 1496 cm^{-1} are in good agreement with the calculated bands at 1450 and 1480 cm^{-1} . Furthermore, there are three bands at 1017, 1082, and 1151 cm^{-1} that may be associated with the IR bands at 1013, 1092, and 1166 cm^{-1} . Finally, the Raman spectrum reveals one band at 472 cm^{-1} which

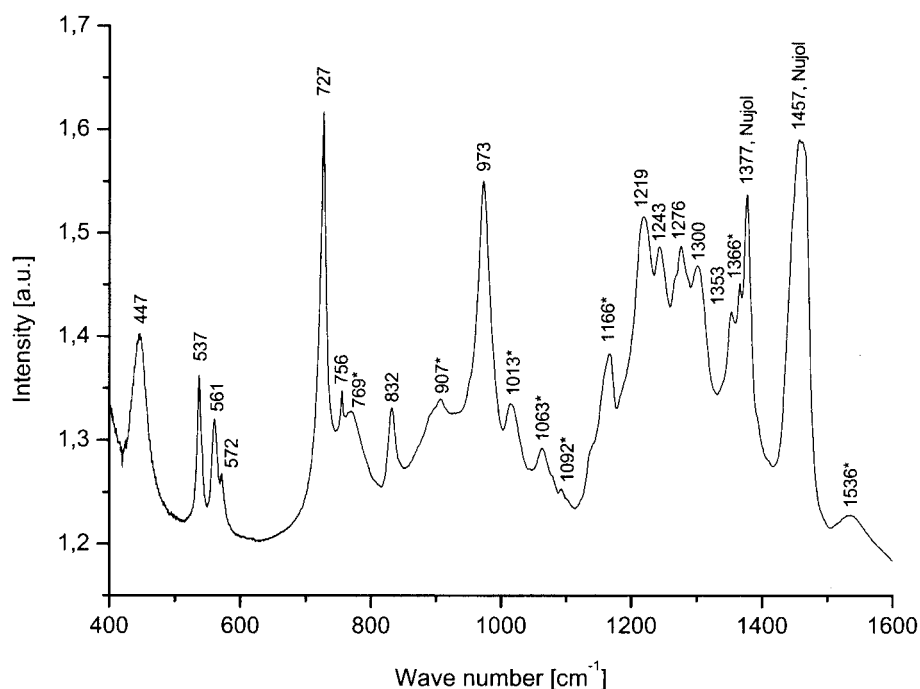


Figure 2. IR spectrum of **1** between 400 and 1600 cm^{-1} (CsI plates, Nujol) with cation bands at $\tilde{\nu} = 769, 907, 1013, 1063, 1092, 1166, 1366$, and 1536 cm^{-1} (marked with *).

Table 3. Comparison of the experimental anion bands of **1** and **2** with anion bands of $[\text{NEt}_4][\text{Al}\{\text{OC}(\text{CF}_3)_3\}_4]^{[22]}$ and calculated frequencies.

| $[\text{H}(\text{OEt}_2)_2][\text{Al}\{\text{OC}(\text{CF}_3)_3\}_4]$ IR | Raman | $[\text{H}(\text{THF})_2][\text{Al}\{\text{OC}(\text{CF}_3)_3\}_4]$ | $[\text{NEt}_4][\text{Al}\{\text{OC}(\text{CF}_3)_3\}_4]$ | $[\text{Al}\{\text{OC}(\text{CF}_3)_3\}_4]^-$ (calcd.) |
|---|-----------|---|---|--|
| 286 (mw) | 228 (w) | — | 286 (mw) | 274 (w) |
| 314 (m) | 289 (w) | — | 316 (m) | 302 (w) |
| 329 (w) | 320 (m) | — | 331 (w) | 320 (w) |
| — | 332 (m) | — | 367 (mw) | 352 (w) |
| 375 (m) | 368 (w) | — | 378 (mw) | 364 (w) |
| 447 (ms) | 381 (vw) | — | 447 (ms) | 420 + 436 (mw) |
| 537 (m) | 537 (m) | 446 (ms) | 537 (m) | 520 (mw) |
| 561 (m) | 564 (w) | 537 (m) | 562 (mw) | 546 (mw) |
| 572 (mw) | 573 (m) | 561 (m) | 571 (w) | 556 (w) |
| 727 (vs) | 744 (s) | 571 (mw) | 727 (s) | 708 (m) |
| 756 (m) | 798 (s) | 727 (vs) | 756 (mw) | 736 (w) |
| 832 (m) | 828 (w) | 755 (m) | 833 (m) | 816 (w) + 826 (w) |
| 973 (vs) | 975 (w) | 831 (m) | 973 (s) | 962 (s) |
| — | — | 973 (vs) | — | 1112 + 1138 (w) |
| 1219 (s) | 1216 (vw) | — | 1217 (vs) | 1216 (vs) |
| 1243 (s) | 1243 (vw) | 1220 (s) | 1240 (s) | 1230 (vs) |
| — | — | 1242 (s) | 1254 (s) | — |
| 1276 (s) | 1278 (m) | — | 1277 (vs) | 1260 (vs) |
| 1300 (s) | 1312 (w) | 1276 (s) | 1299 (s) | — |
| 1353 (ms) | — | 1300 (s) | 1353 (ms) | 1344 (vs) |
| | | 1353 (ms) | | |

Table 4. Experimental cation bands of **1** compared to $[\text{H}(\text{OEt}_2)_2][\text{CHB}_{11}\text{H}_5\text{Cl}_6]$ (**cb**) and calculated frequencies as well as free Et_2O .

| Compound 1 (exp.) IR | Raman | cb ^[7] (exp.) | $[\text{H}(\text{OEt}_2)_2]^+$ (calcd.) ^[a] Spectrum | Assignment | Et_2O ^[25] (exp.) | Et_2O (calcd.) |
|--------------------------------|----------|---------------------------------|--|------------|--|--------------------------------|
| | 472 (w) | | 480 (vw) | O–H–O | 677 | |
| 769 (mw) | | | 774 (w) | O–H–O, C–O | 793 | 810 |
| 907 (mw) | | 925 (vs) | 896 + 914 (ms) | C–O, C–C | 932 | 932 |
| 1013 (m) | 1017 (m) | | 1006 (m) | C–O, C–C | 1025 | |
| 1063 (mw) | 1082 (w) | | 1064 (m) | O–H–O, C–O | 1044 | 1042 |
| 1092 (w) | | | 1071 (vw) | O–H–O, C–C | 1074 | 1072 |
| | 1151 (m) | | 1134 (w) | C–O, C–C | 1119 | 1152 |
| 1166 (ms) | | | 1172 (m) | O–O, C–C | 1150 | 1170 |
| ^[b] | | | 1282 (ms) | C–H | 1296 | |
| 1366 (m) | | | 1370 (mw) | C–H | 1378 | 1368 |
| ^[c] | | | 1426 (mw) | O–H–O, C–H | | 1422 |
| | 1467 (m) | | 1450 (vw) | C–H | | |
| | 1496 (w) | | 1480 (vw) | O–H–O, C–H | | |
| 1536 (mw) | | 1524 (s) | 1536 (s) | O–H–O | 1547 | |
| ^[c] | 2859 (m) | | | C–H | | |
| ^[c] | 2894 (m) | 2872 (w) | | C–H | 2777 | 2838 |
| ^[c] | 2912 (m) | 2907 (w) | 2968 (mw) | C–H | 2807 | 2852 |
| ^[c] | 2948 (s) | 2938 (m) | 3046 (w) | C–H | 2856 | 2870 |
| ^[c] | 2961 (s) | 2984 (s) | 3068 (w) | C–H | 2929 | 2954 |
| ^[c] | 3006 (m) | 3000 (m) | 3070 (w) | C–H | 2972 | 3044 |

[a] Only the maxima of the (deposited) simulation are given. [b] Overlapped by strong anion bands. [c] Overlapped by Nujol bands.

matches with the calculated frequency at 480 cm^{-1} . This frequency refers to a vibration of the oxygen atoms of the cation. All cation bands are shown in Table 4 and are compared to several experimental IR bands as well as selected calculated frequencies.

Figure 3 shows a section of the IR spectrum of **2** between 400 and 1500 cm^{-1} . Again, the typical bands of the perfluorinated *tert*-butoxyaluminate anion are clearly visible (Table 3), as discussed above. Similarly, the position of the

bands relative to the calculated frequencies and the NEt_4^+ salt indicates a distinct salt structure, which is proved by the solid-state structure (Figure 5).

In Figure 3, the bands at $\tilde{\nu} = 603, 775, 894, 918, 1043, 1167, 1365$, and 1448 cm^{-1} can be assigned to vibrations of the cation. Table 5 shows the experimental bands compared to the carboranate anion of Reed,^[7] the maxima of the simulated calculated cation spectrum, as well as experimental^[25] and calculated bands of free THF in a range from

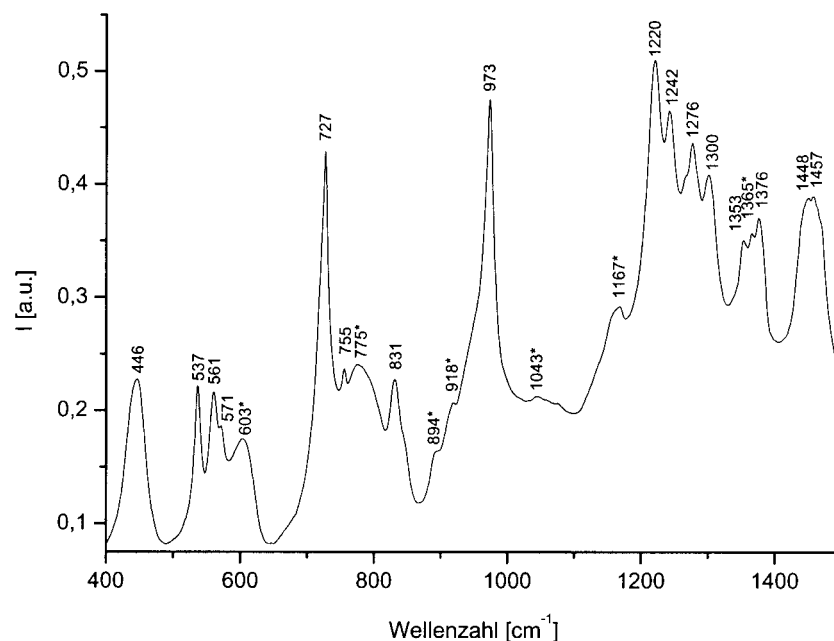


Figure 3. Section of the IR spectrum (CsI, Nujol) of **2** with cation bands at $\tilde{\nu} = 603, 775, 894, 918, 1043, 1167, 1365$, and 1448 cm^{-1} (*).

Table 5. Experimental cation bands of **2** compared to $[\text{H}(\text{THF})_2][\text{CHB}_{11}\text{H}_5\text{Br}_6]$ (**cb**) and calculated frequencies as well as free THF.

| Compound 2 (exp.) | cb ^[7] (exp.) | $[\text{H}(\text{THF})_2]^+$ (calcd.) ^[a] | THF ^[25] (exp.) | THF (calcd.) |
|------------------------------|---------------------------------|--|----------------------------|--------------|
| 603 (ms) | — | 608 (m) | 660 | 630 |
| 775 (m) | — | 794 (m) | | 788 |
| | — | 826 (w) | | 852 |
| 894 (w) | — | 836 (vw) | | 894 |
| 918 (w) | — | 904 (w) | 920 | 932 |
| ^[b] | — | 956 (m) | | 952 |
| 1043 (w) | 1048 (vs) | 986 (w) | 1025 | 1032 |
| — | — | — | 1090 | 1088 |
| [1155 (sh) ?] | — | 1136 (m) | | 1120 |
| [1167 (ms) ?] ^[b] | — | 1156 (vw) | 1175 | 1180 |
| [1220 (vs) ?] ^[b] | — | 1214 (vs) | 1205 | 1194 |
| — | — | — | | 1222 |
| [1242 (s) ?] ^[b] | — | 1240 (s) | 1240 | 1234 |
| ^[b] | — | 1300 (mw) | | |
| 1366 (m) | — | 1326 (w) | | 1322 |
| ^[b] | — | 1346 (w) | 1370 | 1361 |
| ^[c] | — | 1414 (vs) | | |
| 1448 (w) | — | 1444 (w) | 1455 | 1446 |
| 1507 (w, br.) | — | 1514 (m) | | |
| 1517 (w, br.) | — | 1554 (w) | | |
| ^[c] | 2880 (m) | | 2685 | 2868 |
| ^[c] | 2909 (m) | 2976 (w) | | |
| ^[c] | 2933 (w) | 2992 (w) | 2860 | 2986 |
| ^[c] | 2954 (m) | 2998 (w) | 2975 | 3018 |
| ^[c] | 2988 (m) | 3066 (w) | | 3044 |

[a] Only the maxima of the (deposited) simulation are given. [b] Overlapped by strong anion bands. [c] Overlapped by Nujol bands.

700 to 3000 cm^{-1} . Compared to the calculated frequencies, the experimental bands match well; however, the expected bands at $726, 1212, 1312$, and around 3000 cm^{-1} are again overlapped by strong anion or Nujol bands.

Solid-State Structures

The solid-state structure of **1** was determined, confirming the NMR spectroscopic data and showing an ionic lattice

containing $[\text{H}(\text{OEt}_2)_2]^+$ and $[\text{Al}\{\text{OC}(\text{CF}_3)_3\}_4]^-$. The molecular structure of one formula unit is shown in Figure 4.

For the anion, typical structural parameters to those reported earlier^[12] were found. In contrast to the anion, the structural parameters of the cation show some interesting details: the position of the (O)H atom was found in the difference Fourier map and suggests the presence of an unsymmetrical O—H \cdots O bond with an O—O separation of 242.4 pm (cf. 240 to 245 pm in other $[\text{H}(\text{OEt}_2)_2]^+$

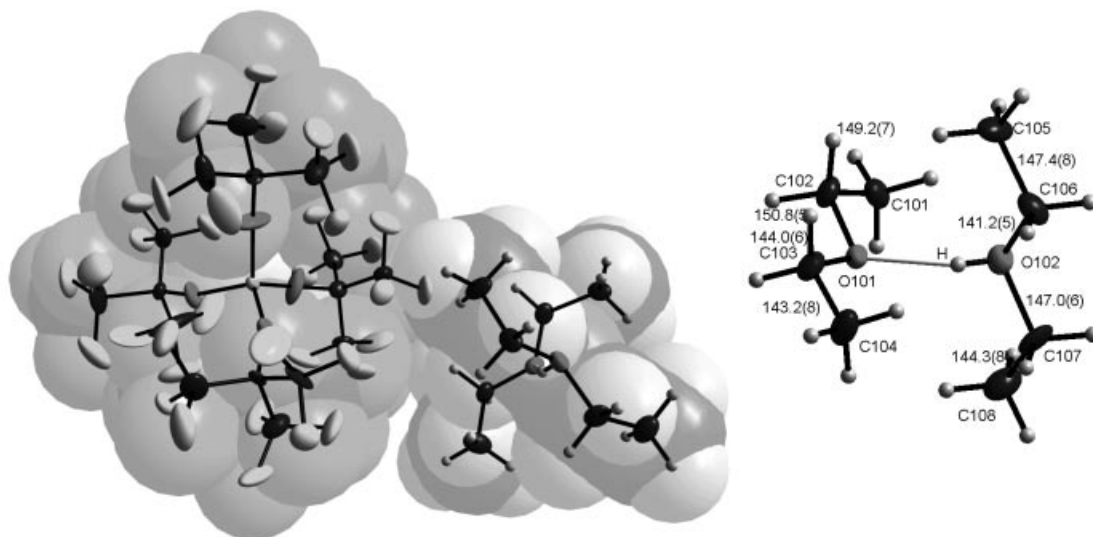


Figure 4. Section of the solid-state structure of **1**. Superposition of a space-filling (light gray) and a thermal ellipsoid model drawn at the 25% probability level.

salts^[4,7,10]). No disorder was evident from the structure. The asymmetric coordination also followed from the C–O bond lengths: compared to free solid diethyl ether,^[26] which has an average O–C bond length of 142.8 pm the average C–O separations of the diethyl ether molecules are elongated by 5.6 (coordinated ether) and 1.3 pm (protonated ether; $\Delta d = 4.3$ pm). This implies that the two diethyl ether molecules in **1** are different and, since the C–O bonds of the coordinated diethyl ether molecules of our oxonium acid are elongated unsymmetrically, the proton is presumably located at one of the two molecules.

The solid-state structure of **2** was also determined by X-ray crystallography. The NMR spectroscopic data could be confirmed as well as the existence of an ionic lattice of $[\text{H}(\text{THF})_2]^+$ and $[\text{Al}\{\text{OC}(\text{CF}_3)_3\}_4]^-$. However, the quality of the data does not allow for extensive discussions and the structure is mainly seen as additional evidence for the na-

ture of **2** being a salt of $[\text{H}(\text{THF})_2]^+$. The acidic proton was not located in the difference Fourier map and is, therefore, not shown. Figure 5 shows one formula unit of the molecular structure.

On the Structure of $[\text{H}(\text{OEt}_2)_2]^+$

It is clear from first principles as well as the DFT calculations of the structures of H-OEt_2^+ vs. symmetric $[\text{H}(\text{OEt}_2)_2]^+$ in Table 6 that the protonation of the oxygen atom should lead to an elongation of the adjacent C–O bonds. However, if this is true, the acidic proton in **1** is attached to the wrong oxygen atom. Still, a similar unsymmetrical elongation with the apparently wrong oxygen atom protonated also occurs for Jutzi's acid $[\text{H}(\text{OEt}_2)_2][\text{B}(\text{C}_6\text{F}_5)_4]$ ($\Delta d = 4$ pm).^[4] A closer analysis shows that the two C–O bond lengths in the nonprotonated diethyl ether molecule are not similar but differ greatly (144.0 vs. 150.8 pm in **1** and 146.6 vs. 154.2 pm in Jutzi's acid). On the other hand, there are two reports of a symmetrically bridged proton in the center of two Et_2O molecules.^[2,10] In these cases all four C–O bond lengths are similar and amount to approximately 146 pm. These initial observations suggest that the position of the proton as determined by X-ray diffraction is unreliable and should not be used for the discussion of a symmetrical or unsymmetrical H-bridge. The C–O and C–C bond lengths were determined with much higher accuracy and should, therefore, be used for the comparison. However, although five crystal structures of $[\text{H}(\text{OEt}_2)_2]^+$ have been published,^[2,4,7–9] hitherto nobody has analyzed the structures in detail. Therefore, the structural parameters of all published $[\text{H}(\text{OEt}_2)_2]^+$ solid-state structures as well as the DFT-calculated parameters of Et_2O , $[\text{HOEt}_2]^+$, and symmetrical $[\text{H}(\text{OEt}_2)_2]^+$ are collected in Table 6.

An analysis of Table 6 underlines the conclusion that the experimentally determined positions of the acidic protons

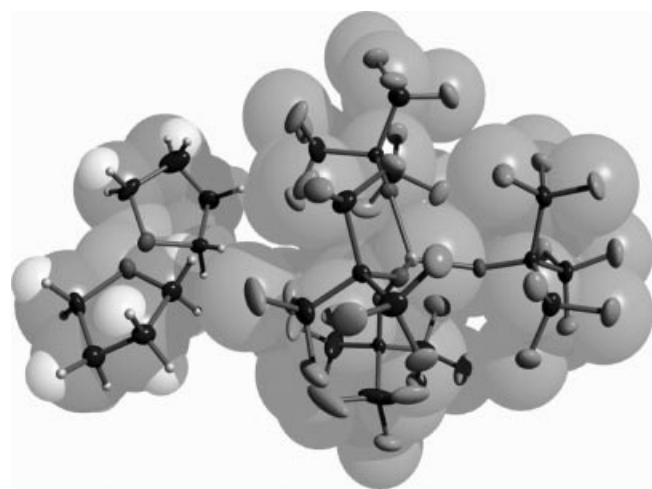
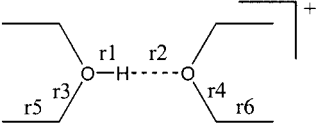


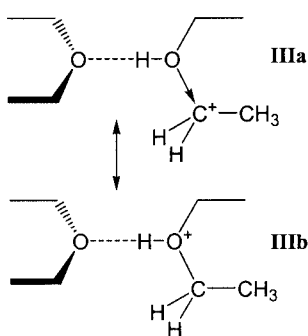
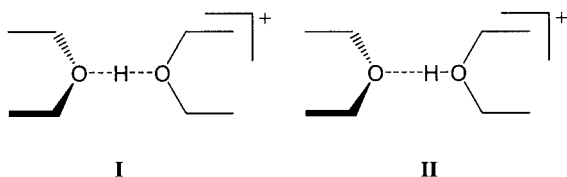
Figure 5. Section of the solid-state structure of **2**. Superposition of a space-filling (pale gray) and a thermal ellipsoid model drawn at 25% probability level.

Table 6. Comparison of the experimental and BP86/TZVPP calculated structural parameters of OEt_2 , $[\text{HOEt}_2]^+$ and $[\text{H}(\text{OEt}_2)_2]^+$ (labeling according to the formula given below. In the asymmetrical case, the two sets of r3 to r6 distances are given).


| Parameter | OEt_2 (exp./calcd.) | $[\text{HOEt}_2]^+$ (calcd.) | $[\text{H}(\text{OEt}_2)_2]^+$ (calcd.) | I | A ^{[2][a]} | B ^{[8][b]} | C ^{[7][c]} | D ^{[4][d]} | E ^{[10][e]} |
|------------|------------------------------|------------------------------|---|----------------|----------------------------|----------------------------|----------------------------|----------------------------|-----------------------------|
| Type | – | – | sym. | asym. | Sym. | asym. | asym. | asym. | sym. |
| r1/r2 [pm] | – | 98.0 | 121.9/122.4 | asym. (80/170) | (116/124) | (111/134) | (108/154) | (93/152) | (119/121) |
| r3 [pm] | – | 152.7 | 147.7 | 141.2/147.0 | 145.5 | 144.8/145.6 | 146.1/150.5 | 142.9/144.3 | f) |
| r4 [pm] | 142.8/142.4 | – | 147.7 | 144.0/150.8 | 146.5 | 144.1/152.4 | 144.6/154.4 | 146.6/154.2 | 144.6 |
| r5 [pm] | – | 149.9 | 151.1 | 144.3/147.4 | 149.0 | 148.2/147.8 | 142.1/144.6 | 138.8/140.7 | f) |
| r6 [pm] | 150.6/151.8 | – | 151.1 | 143.2/149.2 | 147.8 | 126.7/147.6 | 140.3/149.0 | 138.7/145.9 | 144.4 |

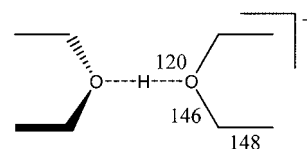
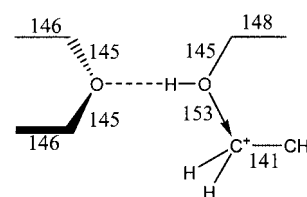
[a] **A** = $[\text{H}(\text{OEt}_2)_2][\text{Zn}_2\text{Cl}_6]$. [b] **B** = $[\text{H}(\text{OEt}_2)_2][(\text{F}_5\text{C}_6)_3\text{B}-\text{C}_3\text{H}_2\text{N}_2-\text{B}(\text{C}_6\text{F}_5)_3]$. [c] **C** = $[\text{H}(\text{OEt}_2)_2][\text{CB}_{11}\text{H}_6\text{X}_6]$. [d] **D** = $[\text{H}(\text{OEt}_2)_2][\text{B}(\text{C}_6\text{F}_5)_4]$. [e] **E** = $[\text{H}(\text{OEt}_2)_2][\text{F}_4\text{C}_6\text{B}(\text{C}_6\text{F}_5)_2\text{OMe}]$. [f] This side of the cation was disordered and, therefore, bond lengths are less accurate and not included.

are unreliable; however, this is common knowledge. More importantly, one realizes from Table 6 that, when concentrating on the C–O and C–C separations, the nature of the H-bridge in $[\text{H}(\text{OEt}_2)_2]^+$ may not simply be reduced to symmetric (**I**) or asymmetric (**II**) but that in the asymmetric case further rearrangements of the structure occur (**IIIa,b** in Scheme 1).

Scheme 1. Possible structures of $[\text{H}(\text{OEt}_2)_2]^+$.

In structure type **II** the C–O bond lengths of the protonated diethyl ether molecule should be symmetrically elongated. This is obviously not the case (Table 6) and therefore structure **III** is important; resonance form **IIIa**, which formally may be viewed as ethanol coordinated to an ethyl cation, accounts for the unsymmetrical C–O bond lengths of the protonated diethyl ether molecule. From the two symmetric and four asymmetric structures in Table 6 one may therefore extract average structural parameters for **I**

and **III**; a schematic representation of the parameters of both forms is given in Scheme 2. A detailed description of the procedure to obtain the average structural data is available as Supporting Information

Symmetrically bridged cation **I**
structures: **A**, **E**Asymmetric cation **III**
structures: **1**, **B**, **C**, **D**Scheme 2. Average structural parameters of **I** and **III** [pm] extracted from the solid-state structures in Table 6.

The structure of **I** is in very good agreement with that predicted on the basis of the BP86/TZVPP calculations (Table 6). However, regardless of whether one starts with a slightly asymmetric or strongly asymmetric structural type **III** the DFT calculations (gas phase!) always lead to the symmetric structure type **I**. Nevertheless, the average structural parameters of **III** in Scheme 2 are likely and may be compared to related moieties: the short C–C bond length of 141 pm of the formal ethyl cation in **III** may be compared to the BP86/SV(P)-optimized distances of the free ethyl cation (141.2 pm), free ethane (153.1 pm), and the base-stabilized ethyl cations $\text{D} \rightarrow {}^+\text{CH}_2\text{CH}_3$ [**D** = OH_2 , $d(\text{C}-\text{C}) = 150.0$ pm; **D** = OMe_2 , $d(\text{C}-\text{C}) = 150.7$ pm]. The

formal donor–acceptor C–O bonds in the $D \rightarrow {}^+CH_2CH_3$ cations are 156.3 pm (H_2O) and 152.9 pm (OMe_2), in good agreement with our estimate of 153 pm in **III**. All other distances are normal. The data in Scheme 2 may not be taken as absolute, however, since libration has not been accounted for and the structures may be affected by a superposition of the asymmetric structures **III** (i.e. the site may partly be occupied as $Et_2O \cdots HO^+Et_2$ and partly as $Et_2O^+H \cdots OEt_2$; structure **C**, for example, appears to be afflicted by this type of disorder). However, the general trend of the completely asymmetric structural type **III** holds. Further evidence for this assumption comes from the solid state MAS NMR spectrum of **1**: two lines at $\delta = 71.1$ and 71.7 ppm were observed for the OCH_2 groups of the diethyl ether molecules. This again points to an asymmetric coordination in the solid state and supports the formulation of structure **III**. Thus, it appears likely that forms **I** and **III** may be stable in the solid state and the final decision as to which isomer is formed is governed by subtle differences of the anion–cation contacts of the different salts in the solid state. Moreover, it is evident that the discussion of the nature of the short- strong- and low-barrier H-bonds in $[H(OEt_2)_2]^+$ may not be reduced to the question of a symmetrical ($O \cdots H \cdots O$) or asymmetrical ($O-H \cdots O$) H-bond. If an asymmetrical H-bond is formed, this leads to a further rearrangement of the structure of the $[H(OEt_2)_2]^+$ cation, which may be described by the resonance structures **IIIa,b**.

Conclusions

A facile preparation of **1** and **2** as stable salts of the oxonium acids $[H(OEt_2)_2]^+$ and $[H(THF)_2]^+$ has been achieved. Both compounds were fully characterized by experimental and quantum chemical methods; they are strongly Brønsted acidic reagents. Due to the facile preparation, the commercial availability of $Li[Al(OR)_4]$, the good thermal solution stability (especially of **1**), and the weakly coordinating and chemically robust nature of the $[Al(OR)_4]^-$ counterion, **1** is an attractive reagent for synthesis, particularly in organometallic chemistry and homogeneous catalysis (for applications of $[H(OEt_2)_2]^+$ salts see ref.^[4–11]). Interestingly, the solid-state structure of **1** includes an asymmetrically bridging H-atom; symmetric H-bridges have also previously been observed.^[10] A symmetric H-bridge is also the minimum structure of the quantum chemical calculations. From an analysis of all published $[H(OEt_2)_2]^+$ structures we have shown that if an asymmetric H-bridge is formed, this leads to a further rearrangement of the structure and to the structural type **III** in Scheme 2, which is further supported by solid state MAS NMR spectroscopy. This point has hitherto been neglected in the discussion of the nature of short, strong, low-barrier H-bonds, although it should be taken into account. We conclude that the final decision as to the formation of a symmetrical or an unsymmetrical H-bridge is balanced by subtle differences between the anion–cation contacts of the salts in the solid state. Finally, we have been able to revise some erroneously assigned

NMR shifts and give the most complete vibrational characterization of the $[H(OEt_2)_2]^+$ and $[H(THF)_2]^+$ cations currently available.

Experimental Section

General Procedures: Due to the air- and moisture-sensitivity of most materials all manipulations were undertaken using standard vacuum and Schlenk techniques as well as in a glove box with an argon atmosphere (H_2O and $O_2 < 1$ ppm). All solvents were dried by conventional drying agents and distilled afterwards. The solutions of HX ($X = Cl, Br$) in Et_2O and THF were prepared by condensing HX from a flask with known volume and pressure. Solution NMR spectra were recorded in CD_2Cl_2 at room temperature on a Bruker AC 250 spectrometer; data are given in ppm relative to the solvent signals, aqueous $AlCl_3$ (^{27}Al) and CF_3Cl (^{19}F). Solid-state NMR spectra were obtained with a Bruker Avance 500 MHz spectrometer. IR spectra were obtained in nujol mull between CsI plates on a Bruker IFS 66 IR spectrometer, Raman spectra were recorded on a Bruker RFS 100/S Raman spectrometer. The differential temperature analysis measurements were performed with a Netzsch STA 429 DSC/DTA unit. About 20 mg of **1** was used for the experiment; preparation of the measurement and weighing were done in a glove box. The DTA curves were recorded at a heating rate of 5 K min^{-1} .

Preparation of $[H(OEt_2)_2][Al\{OC(CF_3)_3\}_4]$ (1**):** a) $LiAl[OC(CF_3)_3]_4$ (20.02 g, 20.06 mmol) was weighed into a 1-L round-bottomed flask with a glass valve and suspended in a mixture of CH_2Cl_2 (approx. 500 mL) and Et_2O (6.4 mL, 61.7 mmol). The suspension was frozen in liquid nitrogen and HBr (1.746 g, 21.6 mmol) was condensed directly onto the mixture. This mixture was allowed to reach room temperature and stirred overnight; white colloidal LiBr was formed. The LiBr precipitate was filtered off to give a solution of **1** in CH_2Cl_2 . After removing all volatiles in vacuo from the filtrate, pure **1** was isolated as a white powder (21.80 g, 94.8%). Larger crystals were obtained by recrystallization of the powder from a mixture of toluene and diethyl ether (10:1).

b) $LiAl[OC(CF_3)_3]_4$ (0.740 g, 0.76 mmol) was suspended in pure diethyl ether (approx. 30 mL) and gaseous HCl (0.030 g, 0.84 mmol) was condensed directly onto the frozen (77 K) mixture. All other manipulations were undertaken according to the description in part a). Yield: 0.766 g (87%). 1H NMR (250 MHz): $\delta = 1.34$ (t, $^3J_{H,H} = 7.138$ Hz, 12 H), 3.90 (br., 8 H), 14.68 (br., 1 H) ppm. $^{13}C\{^1H\}$ NMR (63 MHz): $\delta = 13.8$ (s), 69.3 (s), 121.5 (q, $^1J_{C,F} = 292.2$ Hz) ppm. ^{19}F NMR (235 MHz): $\delta = -75.43$ (s) ppm. ^{27}Al NMR (78 MHz): $\delta = 36$ (s). IR (CsI plates, Nujol): $\tilde{\nu} = 206$ (mw), 286 (mw), 314 (m), 375 (m), 447 (ms), 537 (m), 561 (m), 572 (mw), 727 (vs), 756 (m), 769 (mw), 832 (m), 907 (mw), 973 (vs), 1013 (m), 1063 (mw), 1166 (ms), 1219 (s), 1243 (s), 1276 (s), 1300 (s), 1353 (ms), 1366 (ms), 1377 (s), 1457 (vs), 1536 (mw) cm^{-1} .

Preparation of $[H(THF)_2][Al\{OC(CF_3)_3\}_4]$ (2**):** $LiAl[OC(CF_3)_3]_4$ (0.700 g, 0.719 mmol) was weighed into one side of a two-bulb, frit-plate flask with a glass stem that was closed with two greaseless Young valves, and suspended in CH_2Cl_2 (approx. 30 mL). On the opposite side, HBr (0.95 mL of a 0.834 M solution) dissolved in THF was added with a syringe through a septum. Cooling the suspension to $-80^\circ C$ caused HBr and THF to condense onto the Li salt. The mixture was allowed to reach ambient temperature and stirred for 48 h to form white colloidal LiBr. After removing all volatiles under vacuum, a dark brown oily residue formed from which **2** precipitated as rhombus-shaped crystals in 65% yield. 1H NMR (250 MHz): $\delta = 2.05$ (m, 8 H), 3.95 (m, 8 H), ca. 8 (broad,

1 H) ppm. $^{13}\text{C}\{^1\text{H}\}$ NMR (63 MHz): δ = 25.5 (CH_2), 70.6 (OCH_2), 121.5 (q, $^1J_{\text{C,F}}$ = 291.7 Hz) ppm. ^{27}Al NMR (78 MHz): δ = 36 (s) ppm. IR (CsI plates, Nujol): $\tilde{\nu}$ = 446 (ms), 537 (m), 561 (m), 571 (mw), 603 (ms), 727 (vs), 755 (m), 775 (m), 831 (m), 894 (w), 918 (w), 973 (vs), 1043 (w), 1167 (ms), 1220 (s), 1242 (s), 1276 (s), 1300 (s), 1353 (ms), 1365 (ms), 1376 (ms), 1448 (s), 1457 (s), 1626 (w), 2724 (w), 2853 (ms), 2921 (ms), 2957 (ms) cm^{-1} .

X-ray Structure Determination: Suitable crystals of **1** were formed by cooling a solution in toluene containing a small amount of diethyl ether to 5 °C. Crystals of **2** precipitated directly from the oily residue after removal of all volatiles. Data were collected on a Stoe IPDS II diffractometer using Mo-K_α radiation (λ = 0.71073 Å) at 150 K. Single crystals were mounted in perfluoro ether oil on top of a glass fiber and then placed in the cold stream of a low-temperature device so that the oil solidified. Unit-cell parameters were calculated from a least-squares refinement of the setting angles of 5000 reflections collected. The space groups were identified as $P2_1$ (**1**) and $P2_1/c$ (**2**). The structures were solved with the SIR2002 program^[27] (**1**) or direct methods in SHELXS^[28] (**2**) and successive interpretation of the difference Fourier maps using SHELXL-97. Refinement against F^2 was carried out with SHELXL-97. All non-hydrogen atoms were included anisotropically in the refinement; all hydrogen atoms except the acidic proton in **1** were included isotropically at the calculated positions based on a riding model. The acidic proton in **1** was located in the difference Fourier map and included isotropically in the refinement. The lattice parameters of **1** are very close to being tetragonal (approx. 9, 14, 14 Å; 90, 90, 90°; V = 1950 Å³); in fact, the $[\text{PX}_4][\text{Al}(\text{OR}^F)_4]$ salts ($X = \text{Br}, \text{I}$)^[17b] crystallize with a very similar truly tetragonal cell (approx. 9, 13.5, 13.5 Å; 90, 90, 90°; V = 1850 Å³; $X = \text{I}$). In the latter structures the Al and P atoms reside on special positions with 4 site symmetry and $Z = 2$. When a cation with lower symmetry but similar size crystallizes with the symmetric $[\text{Al}(\text{OR}^F)_4]^-$ anion and the lattice parameters are almost the same, this necessarily leads to twinning, as previously observed when exchanging PX_4^+ for P_2X_5^+ .^[17b] In the

case of **1** the $[\text{H}(\text{OEt}_2)_2]^+$ cation also has less symmetry than PX_4^+ , which implies that the symmetry had to be reduced to at least monoclinic. We were able to solve the structure in the space group $P2_1$ and finally solved the twin law (i.e.: TWIN 0 0 1 0 1 0 0 with BASF 0.43362) that lowered the R_1 value immediately from 15.6% to 4.8%. Relevant data concerning crystallographic data, data collection and refinement details are compiled in Table 7.

CCDC-239426 (for **1**) and -239427 (for **2**) contain the supplementary crystallographic data for this paper. These data can be obtained free of charge from The Cambridge Crystallographic Data Centre via www.ccdc.cam.ac.uk/data_request/cif.

Computational Details: All quantum chemical calculations were carried out with the TURBOMOLE program package.^[29] The geometries of $[\text{H}(\text{OEt}_2)_2]^+$ and $[\text{H}(\text{THF}_2)_2]^+$ were optimized in C_1 symmetry by DFT calculations using the BP86/SV(P)^[30] or BP86/TZVPP^[31] basis sets, as well as RI-MP2 methods using the TZVPP basis set.^[32] Vibrational frequencies were calculated at the BP86/SV(P) level and used to verify the nature of the obtained minima.^[33]

For the estimation of the reaction enthalpies of the formation of compounds **1** and **2**, the oxonium acids as well as a Li cation coordinated by two diethyl ether molecules were calculated by using the same procedure as above. The resulting reaction (2) is isodesmic and inaccuracies arising during the calculation are minimized due to error cancellation. The calculated enthalpies were also corrected for the influences of the Gibbs energy at 298 K (with the semi-empirical PM3 method implemented in Gaussian 98)^[34] as well as solvent effects (COSMO model, CH_2Cl_2 solvent with $\epsilon_r = 8.93$).^[35]

Supporting Information: Simulation of IR spectra based on calculations of vibrational frequencies, Raman spectra, IR spectra (200–700 cm^{-1}), tables of optimized atomic coordinates from density functional calculations, tables for the extracted average structural parameters of **1** and **III** in Scheme 2.

Table 7. Summary of crystallographic data collection for **1** and **2**.

| | 1 | 2 |
|---|--|--|
| Formula | $\text{C}_{24}\text{H}_{21}\text{AlF}_{36}\text{O}_6$ | $\text{C}_{24}\text{H}_{16}\text{AlF}_{36}\text{O}_6$ |
| Temperature [K] | 150 | 150 |
| Crystal system | monoclinic | monoclinic |
| Space group | $P2_1$ | $P2_1/c$ |
| a [pm] | 1405.4 | 965.39(19) |
| b [pm] | 987.6 | 1676.3(3) |
| c [pm] | 1406.5 | 2322.2(5) |
| β [°] | 90.06 | 98.92(3) |
| Volume [nm ³] | 1.9522 | 3.7126(13) |
| Z | 2 | 4 |
| $D_{\text{calcd.}}$ [Mg m^{-3}] | 1.899 | 1.988 |
| Absorption coefficient [mm^{-1}] | 0.263 | 0.276 |
| $F(000)$ | 1100 | 2180 |
| Crystal size [mm ³] | $0.8 \times 0.5 \times 1.0$ | $0.3 \times 0.3 \times 0.4$ |
| θ range for data collection [°] | 6.81 to 21.96 | 6.84 to 24.71 |
| Index ranges | $-14 \leq h \leq 14$ $-10 \leq k \leq 10$ $-14 \leq l \leq 14$ | $-11 \leq h \leq 11$ $-19 \leq k \leq 12$ $-27 \leq l \leq 21$ |
| Reflections collected | 10 013 | 11 548 |
| Independent reflections | 4620 [$R(\text{int.}) = 0.0471$] | 5245 [$R(\text{int.}) = 0.0950$] |
| Data/restraints/parameters | 4620/1/607 | 5245/93/606 |
| Goodness-of-fit on F^2 | 1.039 | 1.095 |
| Final R indices [$I > 2\sigma(I)$] | $R_1 = 0.0482$, $wR_2 = 0.1197$ | $R_1 = 0.1147$, $wR_2 = 0.2939$ |
| R indices (all data) | $R_1 = 0.0513$, $wR_2 = 0.1227$ | $R_1 = 0.1732$, $wR_2 = 0.3311$ |
| Largest diff. peak and hole [e Å^{-3}] | 0.214 and -0.217 | 0.684 and -0.504 |

Acknowledgments

This work was supported by the Deutsche Forschungsgemeinschaft and the Fonds der Chemischen Industrie. We would like to thank Dr. J. Sawatzki of the Bruker demonstration lab for recording the Raman spectrum and Dr. R. Witter and Prof. A. Ulrich for recording the MAS NMR spectra. We are grateful to Prof. H. Schnöckel for many useful discussions.

- [1] G. A. Olah, A. M. White, D. H. O'Brien, *Chem. Rev.* **1970**, *70*, 561.
- [2] S. P. Kolesnikov, I. V. Luyudkovskaya, M. Y. Antipin, Y. T. Strutchkov, O. M. Nefedov, *Bull. Acad. Sci. USSR Div. Chem. Sci. (Engl. Transl.)* **1985**, *34*, 74.
- [3] For recent reviews see: a) C. Reed, *Acc. Chem. Res.* **1998**, *31*, 133; b) S. H. Strauss, *Chem. Rev.* **1993**, *93*, 927; c) I. Krossing, I. Raabe, *Angew. Chem.* **2004**, *116*, 2116; d) E. Y.-X. Chen, T. J. Marks, *Chem. Rev.* **2000**, *100*, 1391.
- [4] P. Jutzi, C. Müller, A. Stämmler, H.-G. Stämmler, *Organometallics* **2000**, *19*, 1442.
- [5] R. Taube, S. Wache, *J. Organomet. Chem.* **1992**, *428*, 431.
- [6] M. Brookhart, B. Grant, A. F. Volpe Jr., *Organometallics* **1992**, *11*, 3920.
- [7] D. Stasko, S. P. Hoffmann, K. C. Kim, N. L. Fackler, A. S. Larsen, T. Drovetskaya, F. S. Tham, C. A. Reed, C. E. Rickard, P. D. Boyd, E. S. Stoyanov, *J. Am. Chem. Soc.* **2002**, *124*, 13 869.
- [8] D. Vagedes, G. Erker, R. Fröhlich, *J. Organomet. Chem.* **2002**, *641*, 148.
- [9] S. J. Lancaster, A. Rodriguez, A. Lara-Sanchez, M. D. Hannant, D. A. Walker, D. H. Hughes, M. Bochmann, *Organometallics* **2002**, *21*, 451.
- [10] L. D. Henderson, W. E. Piers, G. J. Irvine, R. McDonald, *Organometallics* **2002**, *21*, 340.
- [11] a) L. H. Shultz, M. Brookhart, *Organometallics* **2001**, *20*, 3975; b) L. K. Johnson, C. M. Killian, M. Brookhart, *J. Am. Chem. Soc.* **1995**, *117*, 6414; c) J. Cámpora, J. A. López, P. Palma, P. Valerga, E. Spillner, E. Carmona, *Angew. Chem.* **1999**, *111*, 199; *Angew. Chem. Int. Ed.* **1999**, *38*, 147; d) G. Kehr, R. Roesmann, R. Fröhlich, C. Holst, G. Erker, *Eur. J. Inorg. Chem.* **2001**, 535; e) D. A. Walker, T. J. Woodman, D. L. Hughes, M. Bochmann, *Organometallics* **2001**, *20*, 3772.
- [12] I. Krossing, *Chem. Eur. J.* **2001**, *7*, 490.
- [13] S. M. Ivanova, B. G. Nolan, Y. Kobayashi, S. M. Miller, O. P. Anderson, S. H. Strauss, *Chem. Eur. J.* **2001**, *7*, 503.
- [14] a) I. Krossing, *J. Am. Chem. Soc.* **2001**, *123*, 4603; b) I. Krossing, L. van Wüllen, *Chem. Eur. J.* **2002**, *8*, 700.
- [15] T. S. Cameron, A. Decken, I. Dionne, M. Fang, I. Krossing, J. Passmore, *Chem. Eur. J.* **2002**, *8*, 3386.
- [16] I. Krossing, *J. Chem. Soc., Dalton Trans.* **2002**, 500.
- [17] a) I. Krossing, I. Raabe, *Angew. Chem.* **2001**, *113*, 4544; *Angew. Chem. Int. Ed.* **2001**, *40*, 4406; b) M. Gonsior, I. Krossing, L. Müller, I. Raabe, M. Jansen, L. van Wüllen, *Chem. Eur. J.* **2002**, *8*, 4475.
- [18] M. Gonsior, I. Krossing, manuscript submitted to *Chem. Eur. J.*
- [19] I. Krossing, A. Bihlmeier, I. Raabe, N. Trapp, *Angew. Chem.* **2003**, *115*, 1569–1572; *Angew. Chem. Int. Ed.* **2003**, *42*, 1531.
- [20] M. Gonsior, I. Krossing, N. Mitzel, *Z. Anorg. Allg. Chem.* **2002**, *628*, 1821.
- [21] I. Krossing, H. Brands, R. Feuerhake, S. Koenig, *J. Fluorine Chem.* **2001**, *112*, 83.
- [22] M. Gonsior, I. Krossing, I. Raabe, manuscript in preparation.
- [23] Some representative examples: a) C. L. Perrin, *Science* **1994**, *266*, 1665; b) M. E. Tuckerman, D. Marx, M. L. Klein, M. Parinello, *Science* **1997**, *275*, 817; c) J.-C. Jiang, Y.-S. Wang, H.-C. Chang, S. H. Lin, Y. T. Lee, G. Niedner-Schatteburg, H.-C. Chang, *J. Am. Chem. Soc.* **2000**, *122*, 1398; d) G. A. Kumar, M. A. McAllister, *J. Am. Chem. Soc.* **1998**, *120*, 3159.
- [24] M. Hesse, H. Meier, B. Zeeh, *Spektroskopische Methoden in der organischen Chemie*, 4th ed., Georg Thieme Verlag, Stuttgart, New York, **1991**.
- [25] <http://webbook.nist.gov/chemistry>.
- [26] D. André, R. Fourme, K. Zechmeister, *Acta Crystallogr., Sect. B* **1972**, *28*, 2389.
- [27] Sir**2002**.
- [28] G. Sheldrick, SHELX software suite, University of Göttingen, Germany.
- [29] a) R. Ahlrichs, M. Bär, M. Häser, H. Horn, C. Kölmel, *Chem. Phys. Lett.* **1989**, *162*, 165; b) M. v. Arnim, R. Ahlrichs, *J. Chem. Phys.* **1999**, *111*, 9183.
- [30] a) A. D. Becke, *Phys. Rev. A* **1988**, *38*, 3098; b) J. P. Perdew, *Phys. Rev. B* **1986**, *33*, 8822.
- [31] K. Eichkorn, F. Weigend, O. Treutler, R. Ahlrichs, *Theor. Chem. Acc.* **1997**, *97*, 119.
- [32] a) F. Weigend, M. Häser, *Theor. Chem. Acc.* **1997**, *97*, 331; b) F. Weigend, M. Häser, H. Patzelt, R. Ahlrichs, *Chem. Phys. Lett.* **1998**, *294*, 143.
- [33] P. Deglmann, F. Furche, R. Ahlrichs, *Chem. Phys. Lett.* **2002**, *362*, 511.
- [34] Gaussian 98, Revision A.11, M. J. Frisch, G. W. Trucks, H. B. Schlegel, G. E. Scuseria, M. A. Robb, J. R. Cheeseman, V. G. Zakrzewski, J. A. Montgomery, Jr., R. E. Stratmann, J. C. Burant, S. Dapprich, J. M. Millam, A. D. Daniels, K. N. Kudin, M. C. Strain, O. Farkas, J. Tomasi, V. Barone, M. Cossi, R. Cammi, B. Mennucci, C. Pomelli, C. Adamo, S. Clifford, J. Ochterski, G. A. Petersson, P. Y. Ayala, Q. Cui, K. Morokuma, P. Salvador, J. J. Dannenberg, D. K. Malick, A. D. Rabuck, K. Raghavachari, J. B. Foresman, J. Cioslowski, J. V. Ortiz, A. G. Baboul, B. B. Stefanov, G. Liu, A. Liashenko, P. Piskorz, I. Komaromi, R. Gomperts, R. L. Martin, D. J. Fox, T. Keith, M. A. Al-Laham, C. Y. Peng, A. Nanayakkara, M. Challacombe, P. M. W. Gill, B. Johnson, W. Chen, M. W. Wong, J. L. Andres, C. Gonzalez, M. Head-Gordon, E. S. Replogle, and J. A. Pople, Gaussian, Inc., Pittsburgh PA, **2001**.
- [35] a) A. Klamt, G. Schürmann, *J. Chem. Soc., Perkin Trans. 2* **1993**, 799; b) A. Schäfer, A. Klamt, D. Sattel, J. Lohrenz, F. Eckert, *Phys. Chem. Chem. Phys.* **2000**, *2*, 2187.

Received: May 25, 2004